Deliverable D 1.5
DEVICES FOR THERMOMECHANICAL TESTS ON SUBSYSTEMS

Document type	**Deliverable D 1.5**
Document Version / Status	**1.4 - First issue**
Primary Authors	**João Pereira, jpereira@civil.uminho.pt, UMINHO**
Distribution Level	**PU (Public)**
Project Acronym	**ATHOR**
Project Title	**Advanced THermomechanical multiscale mOdelling of Refractory linings**
Grant Agreement Number	**764987**
Project Website	**www.etn-athor.eu**
Project Coordinator	**Marc Huger, marc.huger@unilim.fr, UNILIM**
Document Contributors	**Rafael Oliveira, rafael.oliveira@uc.pt, UMINHO** **Marc Huger, marc.huger@unilim.fr, UNILIM** **Ulrich Marschall, Ulrich.Marschall@RHIMagnesita.com, RHI-Magnesita** **Sido Sinnema, sido.sinnema@tatasteeleurope.com, TATASTEEL** **Diana Vitiello, diana.vitiello@unilim.fr, UNILIM**

Change log

History of changes				
Version	**Date**	**Author (Organization)**	**Change**	**Page**
1.0	28.11.2018	João Pereira, Rafael Oliveira (UMINHO)	First version of the D 1.5 deliverable created	all
1.1	21.12.2018	Ulruch Marschall (RHI Magnesita)	Description of the biaxial testing press added	8
1.2	03.01.2019	Rafael Oliveira (UMINHO) Marc Huger (UNILIM)	Description of devices for measurements on the pilot vessel	all
1.3	15.05.2019	Rafael Oliveira (UMINHO) Marc Huger (UNILIM) Diana Vitiello (UNILIM)	Inclusion of all outstanding sections	14-18
1.4	20.05.2019	Marc Huger (UNILIM) João Pereira (UMINHO)	Proof reading	all

European Commission
Horizon 2020
European Union funding
for Research & Innovation

Table of contents

1. Introduction

The present document summarizes the tests and equipment to be used for the thermomechanical characterization and monitoring of refractory masonry subsystems (masonry wallets and a 3D pilot vessel). This document refers to “Task 1.4 - Devices for validation on masonry and vessels” within “WP1 - Improvement of measurements tools”. Besides this introductory section, three additional sections are presented in this document.

Section 2 describes the different experimental campaigns defined to properly characterize the thermomechanical behaviour of refractory masonry under different boundary conditions. This includes tests on: a) compressive behaviour of bricks (both ambient and elevated temperatures); b) uniaxial compression behaviour of masonry walls (elevated temperatures); c) bi-axial behaviour of masonry walls (elevated temperatures).

Section 3 describes the development of the 3D pilot scale steel ladle and the different alternative techniques that can be used to measure its behaviour during the different laboratory tests. Section 4 summarizes the conclusions and considerations to be taken while preparing and performing these tests.

2. Description of devices for thermomechanical characterization of refractory masonry

In this section, different experimental campaigns are presented. These experimental setups and procedures were chosen considering (not in any particular order): a) type of material under study; b) type of thermomechanical properties necessary to properly characterize the behaviour; c) type of data required for modelling purposes; d) time available to perform the tests; e) availability of equipment; and f) amount of material available.

2.1. Thermomechanical characterization of bricks

The characterization of refractory masonry is required for calibration and validation of numerical models and for definition of nonlinear homogenization techniques. The first step is the mechanical characterization of the bricks. Compression tests will be carried out on cylindrical samples extracted from the bricks, under displacement control with a rate of 0,1 mm/s The sample coring and details are presented in Figure 1.

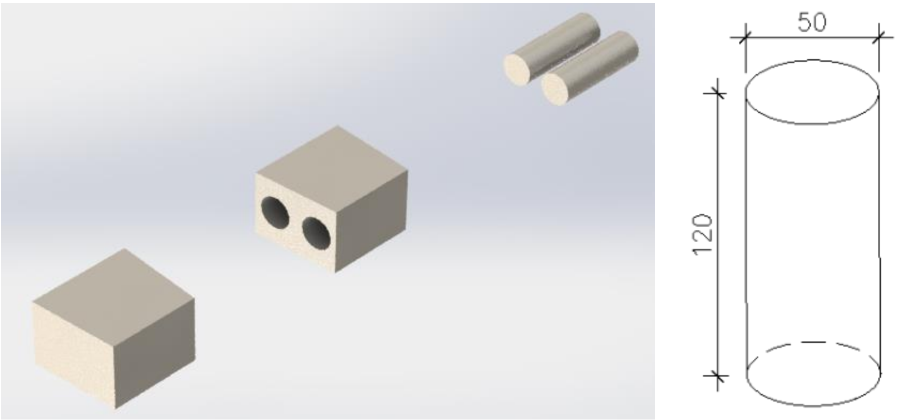

a) b)

Figure 1: Brick samples for compression tests: a) Sample coring, b) Test specimen.

The test setup can be seen in Figure 2. Tests will be performed at both ambient and elevated temperatures (600ºC, 800ºC and 1.000ºC). An electric split furnace will be used to heat the samples at the rate of 5ºC/min. The strains will be measured using a strain gauge at the opening of the furnace and the displacement caused by the press will also be monitored. A 200 kN press with an electromechanical jack will be used to apply the compressive load.

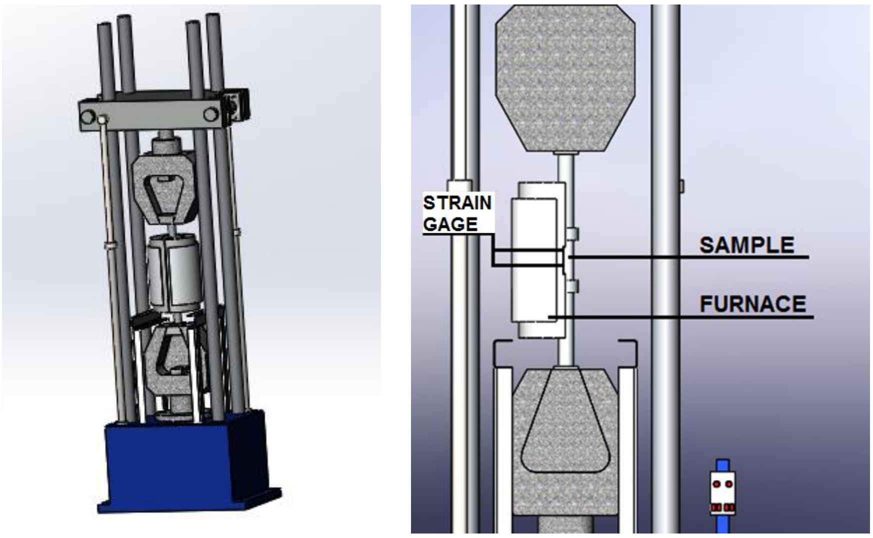

Figure 2: Compression test layout.

Compressive strain-stress curves of the material, as given in Figure 3, are expected to be obtained from these results. It will be possible to identify the compressive strength of the material at room temperature (f_c) and the compressive strength at a given

European Commission | Horizon 2020 European Union funding for Research & Innovation

temperature Θ ($f_{c,\Theta}$). The strain at maximum strength (ε_{c1}) and the ultimate strain (ε_{cu}) may also be determined for each temperature.

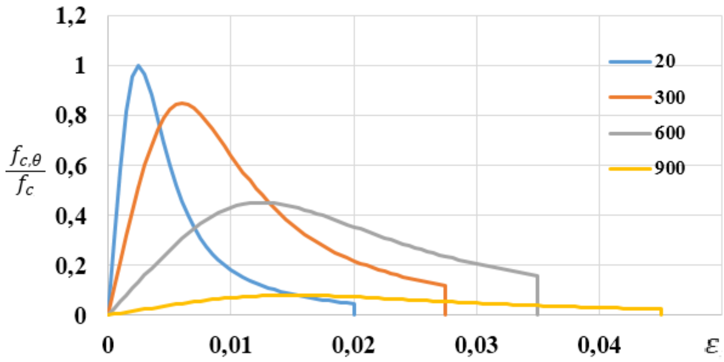

Figure 3: Expected compression results: Strain-stress curves.

2.2. Characterization of dry joints: Triplet Shear Tests

Triplet shear tests will be carried out according to EN 1052-3 to determine the joint behaviour. Three distinct pre-compression levels will be applied to the specimens (20%, 40% and 60%). Two specimens will be prepared for each pre-compression level and for each temperature. The tests will be performed at room temperature, 600ºC and 800 ºC.

The test setup is presented in Figure 4. An HEB500 reaction frame will be used (presented in red), the horizontal pre-compressive load will be applied by a hydraulic jack (RR series 600 kN, presented in yellow) and the vertical shear load will be applied by a hydraulic jack (RR series 750 kN, presented in yellow). An electric vertical furnace (2.10×1.00×0.50m, presented in blue) will be used to heat the samples.

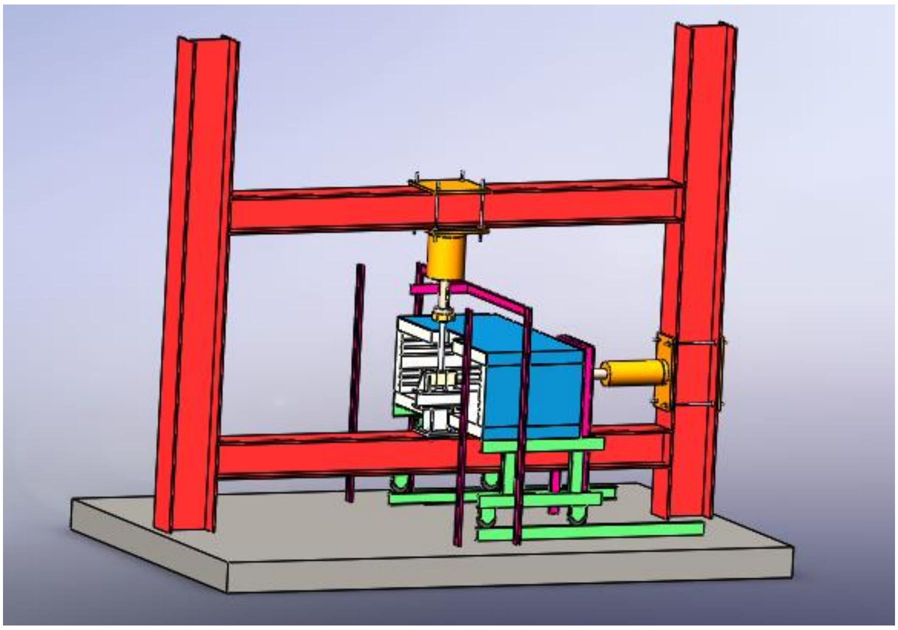

Figure 4: Triplet shear test setup.

One load cell will be installed at each hydraulic jack to measure the force on each jack, as presented in Figure 5. The displacements will be monitored using LVDT's (Linear Variable Displacement Transducer) installed on the piston of each jack. Loads will be transferred using rods in refractory steel, placed at the top opening and lateral opening of the furnace (Figure 6). An internal reaction frame (presented in white) will be designed to place the bricks.

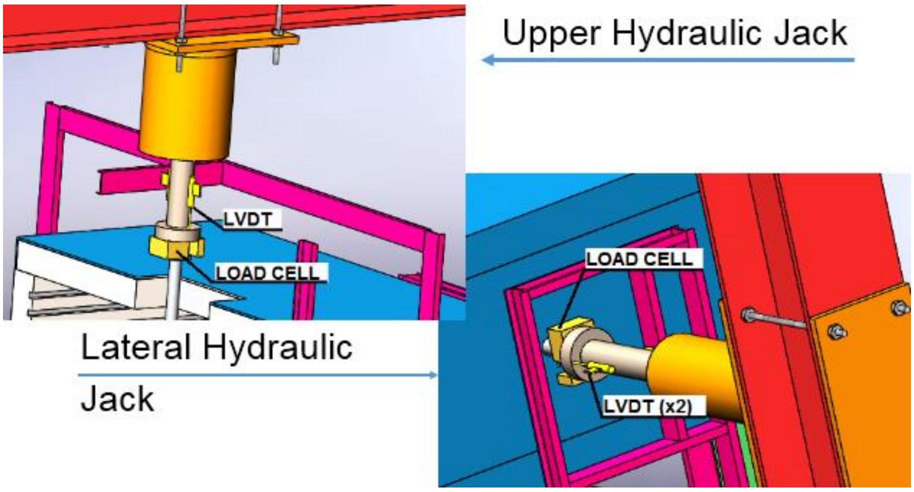

Figure 5: Test setup details for Triplet shear tests – load cells and hydraulic jacks.

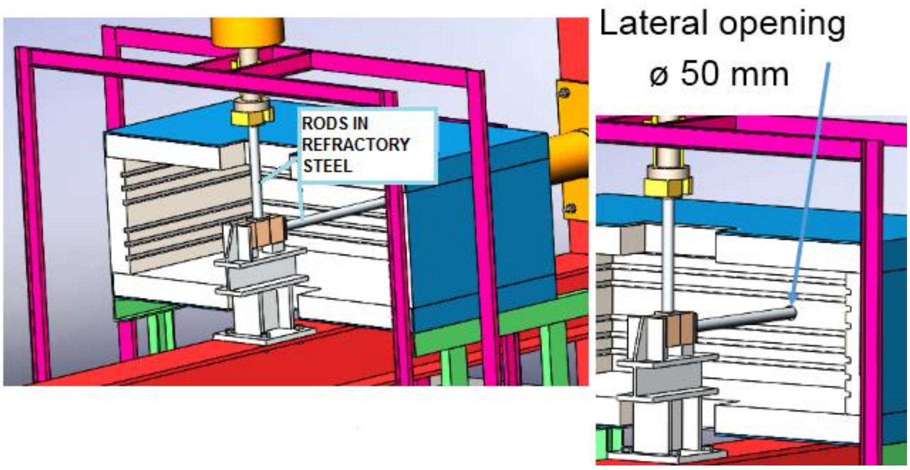

Figure 6: Test setup details for Triplet shear tests – furnace openings and internal reaction frame.

Figure 7 presents the expected result for the triplet shear test. The tests results are registered as pairs of coordinates in the Cartesian plane: normal stress (σ) versus the shear stress (τ). Based on the tests results, it will be possible to determine the initial cohesion (f_{v0}) and the coefficient of friction (μ) of the dry joint. A linear regression will be used to represent a straight line for each temperature, as stated by Mohr-Coulomb formulation:

$$\tau = f_{v0} + \sigma\mu \quad (1)$$

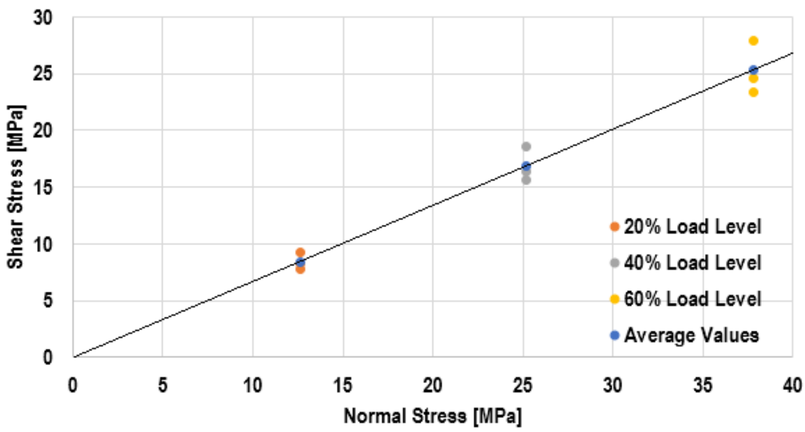

Figure 7: Triplet shear tests - Expected results.

2.3. Uniaxial Compressive tests: masonry wallets

Compressive tests will be performed on refractory walls composed of high content alumina bricks with dry joints at elevated temperatures. High content alumina bricks with the dimensions of 250×124×76 mm will be used. The walls will be six bricks in length and fourteen bricks in height. Therefore, the final dimensions will be 1,500 mm in length by 1,064 mm in height. The test specimens will be placed at a horizontal electric furnace, submitted to a pre-compressive load and then heated under a constant rate. The test setup is presented in Figure 8. An HEB500 reaction frame will be used (presented in red). Two beams will be used to ensure the stiffness required to control the displacements of the hydraulic jack. The pre-compression load will be applied by two hydraulic jacks (RR series 600 kN, presented in yellow). A load application beam (presented in green) will be used to ensure a uniform distribution of the vertical load. An electric vertical furnace (2.10×1.00×1.00m, presented in blue) will be used to heat the wall. A similar test setup has previously been used successfully [1].

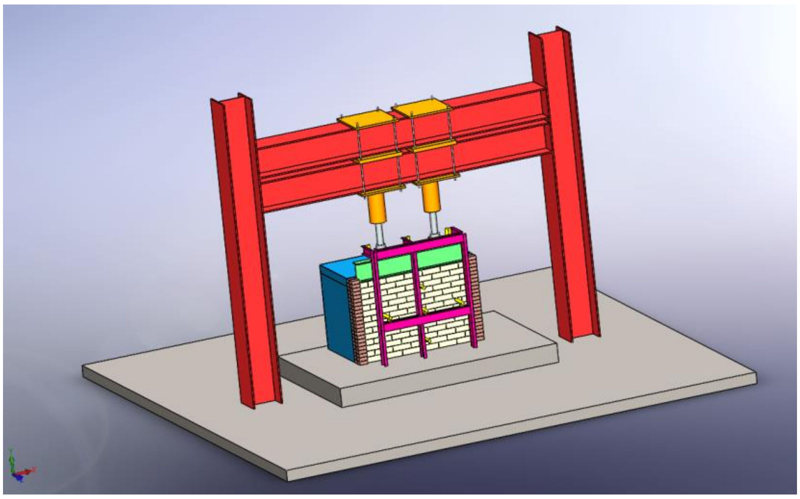

Figure 8: General schematic of the uniaxial compression tests for masonry wallets.

One load cell will be installed at each hydraulic jack to measure the forces applied to the wall, as presented in Figure 9. The vertical displacements at the top of the wall will be monitored using three LVDT's (presented in yellow) installed at the centre, right and left position.

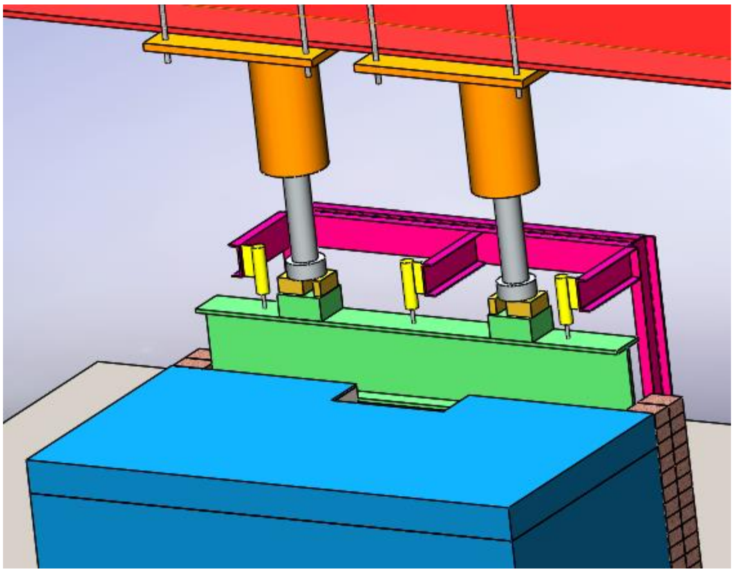

Figure 9: Uniaxial compression test for masonry wallets – detail on load application.

The temperatures field will be measured by type K thermocouples installed at different positions in the wall. To ensure the necessary data for numerical calibration, the thermocouples (TC) will be installed along the thickness of the wall to measure the gradient of temperature. Out-of-plane displacements will be measured at five positions of the wall, including the bottom (1 TC), the centre (3 TC's) and the top (1 TC) (Figure 10). The strain field will be evaluated by the means of the DIC (Digital Image Correlation) technique.

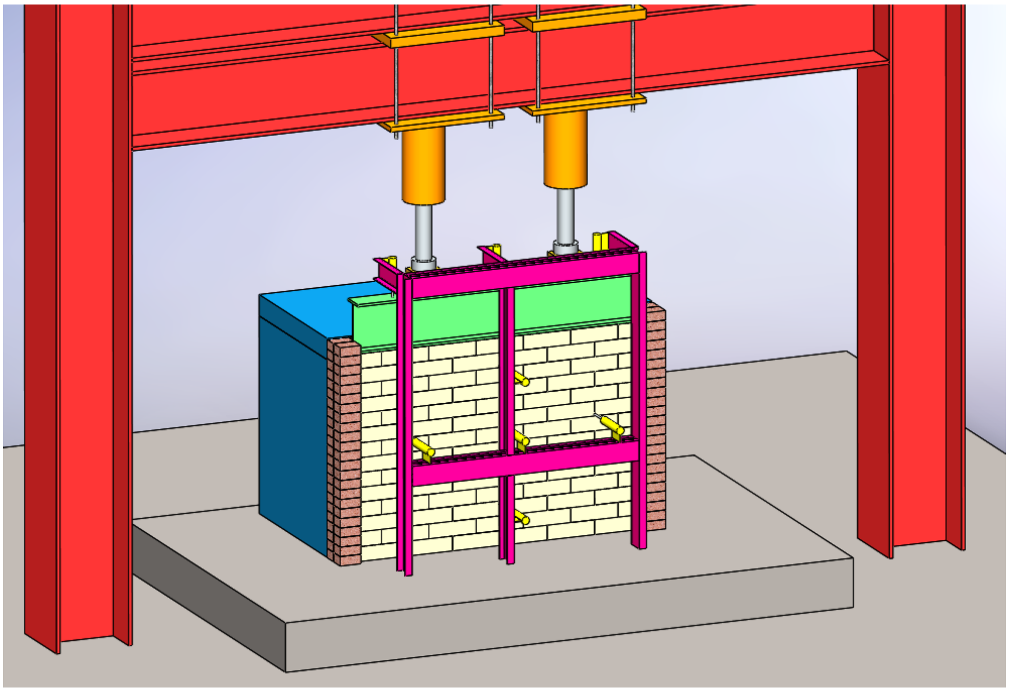

Figure 10: Schematic of the uniaxial compression setup for masonry wallets.

A large set of experimental results is expected. The displacements, strains fields and temperatures fields obtained from the tests will be used for calibration and validation of numerical models and for validation of nonlinear homogenization techniques.

2.4. Biaxial Compressive tests: masonry wallets

The biaxial compressive tests are carried out within a dedicated device based on a previous PhD thesis [2,3]. This provides the possibility to test fields of bricks, similar to a lining wall with a size up to approximately 1.1 x 1.1 meters, by subjecting them to temperatures up to 1500°C. The main part of the testing device, the frame, is shown in Figure 11.

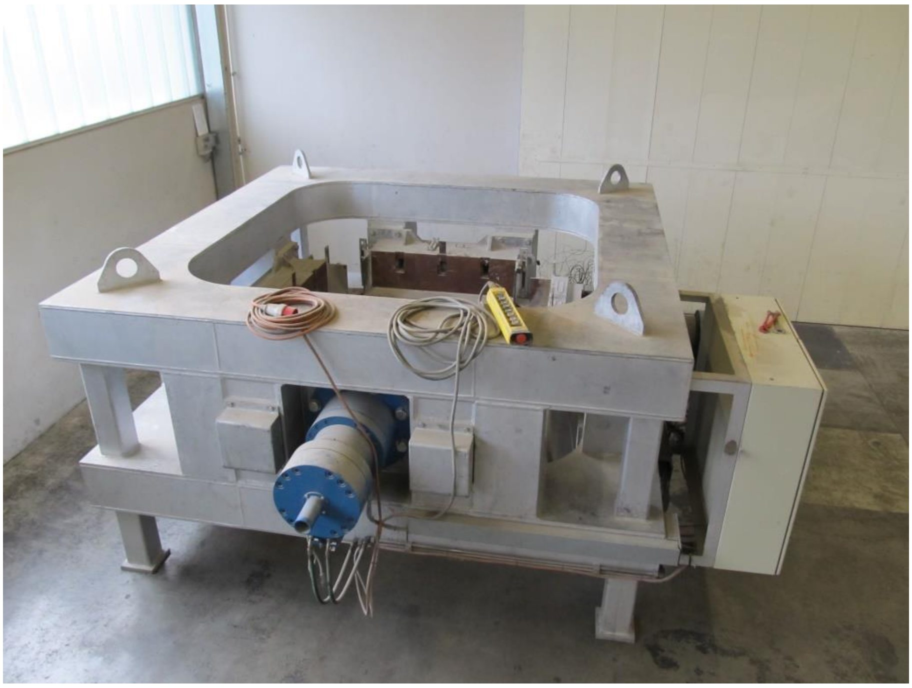

Figure 11: Frame of the biaxial testing press.

Inside this steel frame, an insulating layer of refractory materials will be built on a steel support. On top of this layer, the test field of refractory bricks will be placed. The frame is equipped with four supports which are water cooled. These supports will constrain the testing field using additional high strength refractory materials. Two of them are connected to the steel frame without the possibility to move, the two others, each of them on the opposite side of the steel frame, are equipped with hydraulic jacks. One of them, the blue part in Figure 11, provides the possibility to apply forces to the test field in the two horizontal directions perpendicular to each other.

The test field, including the additional force transmitting refractory materials, will be covered with an electrical heated hood providing the possibility to heat the test field up to 1500°C with an almost uniform temperature distribution in the two horizontal and the vertical direction measured at certain locations with thermocouples.

The stresses generated in the test field are determined by the temperature and the thermal expansion of the refractory material of the test field and the forces applied into the test field by the hydraulic jacks. The displacements within the field will be measured with rod in tube devices in the hot area connected to inductive displacement sensors outside the heating chamber.

3. Description of devices for measurements at the pilot scale steel ladle

3.1. Description of the pilot steel ladle

Thermomechanical pilot scale experiments will be performed with a 3D pilot scale model (Figure 12). It will consist of a cylindrical steel shell with a welded steel bottom. The refractory wall linings will be arranged in concentric layers; the bottom will also consist of layered refractory materials. Since real masonry will be installed, geometrical aspects can be studied within the given pilot scale steel ladle. For instance:

- What effect do joints have on the effective total heat resistance?
- What will be the effect on thermomechanical behaviour of mismatched joints?
- Can the thermomechanical stresses be influenced by the joint thickness or different brick dimensions?

Further, it is possible to measure thermomechanical behaviour of the refractories in the steel ladle. It should be possible to observe creep/plastic deformation under plant circumstances. How the hoop stress in the ring transforms into radial compression of the insulating layer, the damage observed after both first heating and cyclic heating and any wear at the corners of the bricks. It will be also interesting to measure the temperature distribution and fluxes, both for feeding and also validating numerical models being developed.

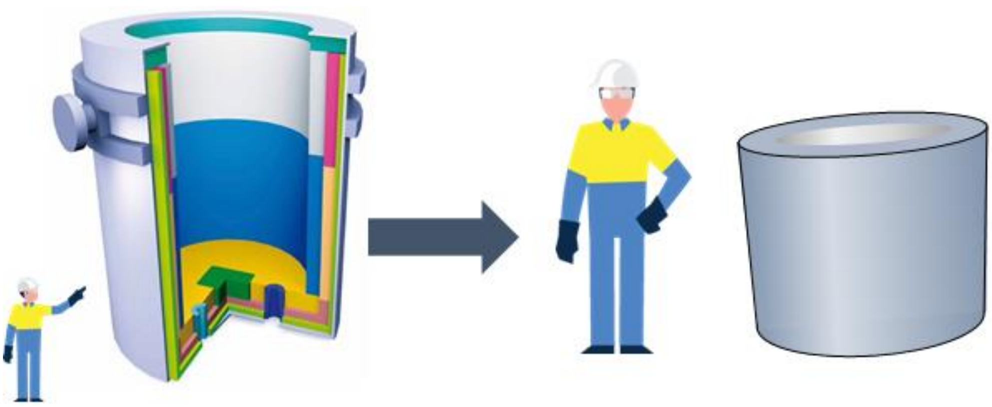

Figure 12: Pilot Steel Ladle.

For the functional design the following considerations have been made:

- The pilot steel ladle will not contain liquid steel, to avoid parasitic effects from it (corrosion, penetration, wear…). The pilot steel ladle will be heated from the center, most likely a radiation tube to prevent oxidation, there will be an adjustable cooling rate of the shell, to control thermal gradient and optional a lid is to be considered. It will consist of a cylindrical steel shell with a welded steel bottom. The typical diameter of the cylinder will be 1,5-2 m (Figure 12).

- Refractory layers will be arranged in the same way as in the full scale ladle (Figure 13), only sizes and shape will be scaled down. The hot face quality (wear lining) will be **Fired spinel brick,** which has excellent resistance against steel, but a high thermal conductivity. The permanent lining will consist of **Fired bauxite brick** with good resistance against steel and a high thermal conductivity. The two insulation layers will be **Grade 26 insulation brick,** temperature resistant up to 1400ºC with a low thermal conductivity and **Microporous insulation** with very low thermal conductivity being temperature resistant up to 1000ºC. Optionally a subset of MgO bricks can be inserted to mimic the slag line refractories configuration.

Figure 13: Example of a real linings application.

3.2. Technologies for measurements in industrial devices

One of the main objectives of developing a 3D pilot model of the steel ladle is to validate technologies, equipment, techniques and protocols to be used at a later stage in the in-situ measurements of the steel ladle in service conditions. This is in fact a very challenging task due to the extreme conditions in which these ladles operate.

Some technologies suitable for application in the industrial devices, and that will be considered for use in the 3D pilot model, were studied and are presented in this section.

3.2.1. Marker Tracking

Marker tracking is an optical method that involves tracking markers installed on the specimen's surface. It can be used to determine both displacement and strain fields during thermomechanical solicitation. It is a powerful technique for strain evaluation: it is simple, fast to use and requires limited computational resources. However, this technique is not able to represent discontinuities on sample, such as cracks.

The marks can be applied on the sample with a felt-tip pen, stamped or painted through a template. The colour of the mark should provide a high contrast with the sample's surface. Stereovision (two or more cameras) may be used to allow measurements of the out-of-plane displacements. Bretagne et al [5] summarize the principles of the technique and the influence of diameter of markers, changes of luminosity, variation of grey level, rotation and out-of-plane displacements in the accuracy of the technique.

3.2.2. Digital Image Correlation

The Digital Image Correlation is an optical full-field measurement technique, it was created at the beginning of the 1980s and has been continuously developed since then, presenting a significant increase in accuracy. It allows the determination of an experimental full-field of strains and displacements, based on the grey level conservation principle [6].

The technique involves recording digital images of a specimen under a mechanical transformation, caused by external forces or temperature variations, and use of software to apply an image correlation algorithm. The recorded images correspond to two different states: a reference state and a deformed state. A speckle pattern will be applied to the sample surface prior to carrying out the test, generating a stochastic pattern of grey shades on the surface, so, each pixel of these images stores a grey value.

The displacement field will be measured based on a virtual grid created in the reference image, this grid defines the subsets of the system. The displacement of each point of this grid is calculated on a subset (D) surrounding the considered point in both states, matching the grey level distribution of the pixels. The DIC principles assumes that:

- the grey level distribution follows the strain of material, therefore, there is a conservation of the optical flow;
- the strains remain homogeneous on the calculus area.

3.2.3. Terrestrial Laser Scanning - 3D Scanning

The Terrestrial Laser Scanners (TLS) were originally developed for as-built modelling of architectural and engineering structures, however they can also be used for high-resolution mapping of terrain, vegetation, and other landscape features over limited distances in the range from 50 m to 300 m, depending on the equipment.

There are different types of laser scanners, but they have the same working principle. A laser scanner emits rapidly pulsing or a continuous laser beam. The head of the equipment rotates around its vertical axis and a mirror rapidly rotates around its horizontal axis (Figure 14 a). The result is a systematic swiping of the laser beam over the scanned area.

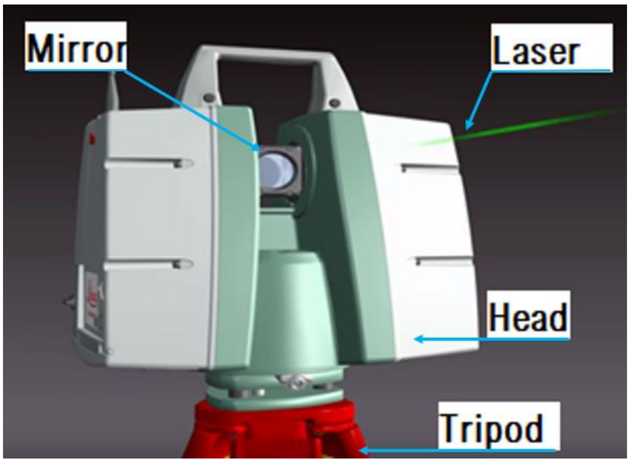

a)

b)

Figure 14: Terrestrial Laser Scanning: (a) Laser emission, (b) Laser return (Source: Leica Geosystems).

When the laser hits an object, part of the laser is reflected back to the scanner. Based on the time between the emission and capture of the beam, it is possible to determine the distance of the object (Figure 14 b). The equipment also records the vertical and horizontal angle of the equipment, allowing the calculation of the position of the point in spherical coordinates, as shown in Figure 15. These coordinates are then converted to Cartesian (X, Y, Z) coordinates and recorded.

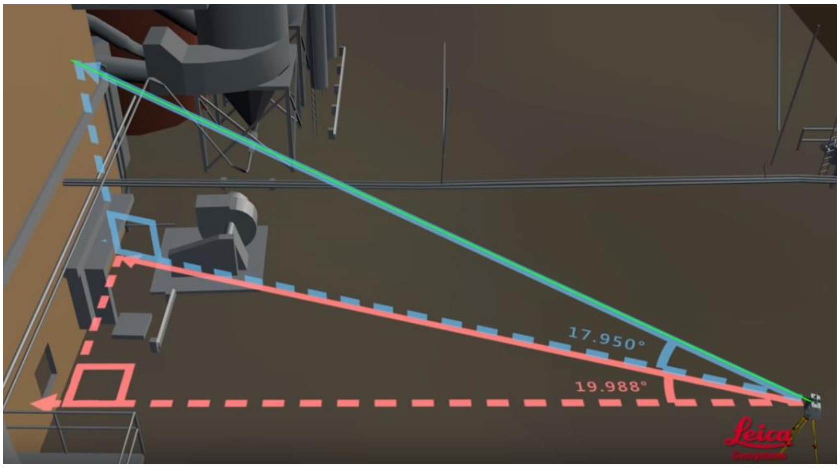

Figure 15: Vertical and horizontal angles (Source: Leica Geosystems).

3.2.4. Photogrammetry

Photogrammetry is the process of generating 3D models from a series of images of the object; the resulting model can be scaled and used to measure distances between objects and to measure the deformed configuration of some structure. This technique provides reliable measurements with a low-cost [7]. It has been successfully used to monitor crack patterns in masonry structures [8], and for structural monitoring [9]. Moreover, this technique was used to evaluate architectural heritage [10-11] and damage to historic structures [12-13]. The use of fisheye lens provides a large Field of View (FOV) that can reach 180º in some cases, reducing the number of image acquisitions and, consequently, saving time in acquisition and processing [14].

Napolitano and Glisic [8] performed experiments in five masonry walls which were damaged in a different way by adjustment of the supports. The damage was monitored using the photogrammetry models, with an accuracy of 0.001 m (Figure 16). The cracks found in the experiments were compared to those found on the numerical models. The authors describe how this method was able to pick the damage conditions for the studied cases.

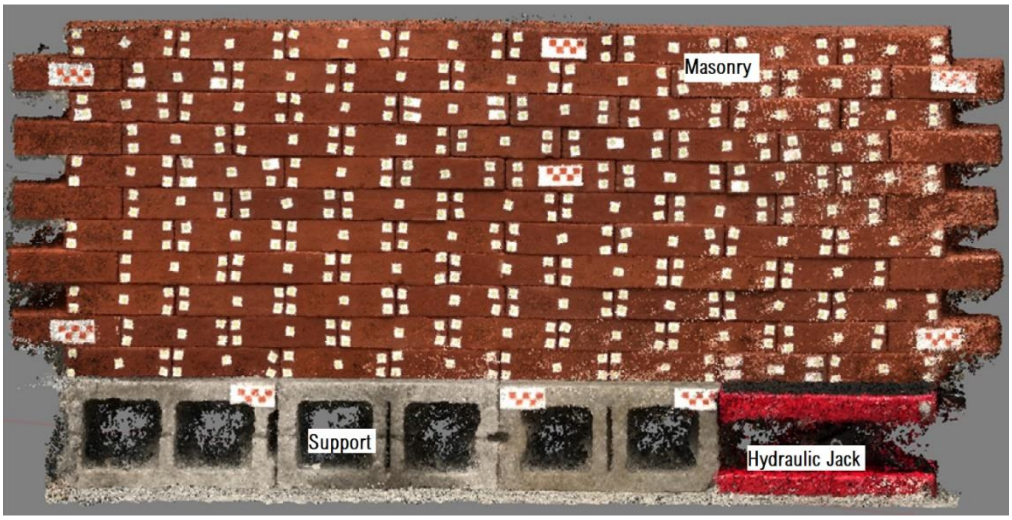

Figure 16: Photogrammetry point cloud for a masonry wall (Source: Napolitano and Glisic, 2019 [8]).

3.3. Measurement of initial imperfections

There are many techniques available for measurements of the initial configuration of the pilot steel ladle. During the fabrication and shipping process, there may be damage caused to the composing elements of the pilot ladle leading to an initial geometrical imperfection. The non-circularity of the steel shell may lead to a non-homogenous stress distribution in the refractory lining and in the shell. Therefore, it is important to have a precise description of the initial geometry of system. The terrestrial laser scanning and the photogrammetry technique are suitable for this application, as they can provide the as-built configuration of the vessel.

Moreover, the steel shell and the refractory lining may present some plastic deformation after cycles of tests. According to the material supplier, the alumina spinel brick has a permanent linear change in dimensions of +0,5% when exposed to temperatures up to 1500ºC. The temperatures will reach those values in the pilot ladle, so it is important to also measure the final state of the system.

3.4. Strain and displacements measurements

The methods presented in Deliverable D1.2 and D1.4 were focused on small scale for laboratory characterization. It is therefore necessary to scale-up these techniques for use with masonry wallets and the pilot steel ladle.

3.4.1. Stereovision

The mark tracking technique is based on the use of two cameras to measure out-of-plane displacements. A calibration process is necessary to define the position and inclination of these cameras. In this procedure, a calibration file with the coordinates of some marks is used to calculate the parameters of location of the cameras (Figure 17).

The out-of-plane displacements of the masonry wallets during heating leads to second order bending effects, so the use of stereovision will be necessary in order to evaluate them. Additionally, the radial displacements in the steel shell leads to a decrease of stresses in the refractory lining. It is important to measure them, as it may help the numerical calibration process. Stereovision is a key instrument in the process of obtaining 3D measurements.

European Commission | Horizon 2020 European Union funding for Research & Innovation

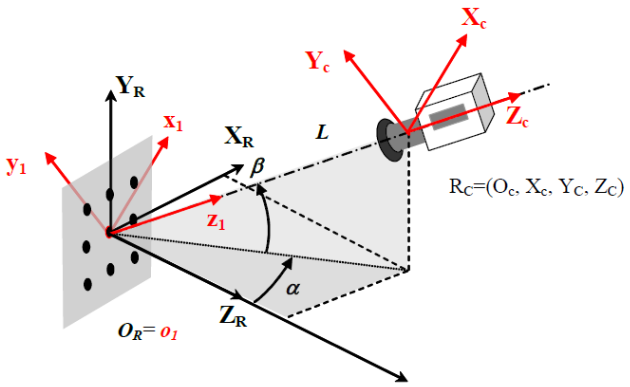

Figure 17: Camera position and inclination (Source: Deftac Handbook).

3.4.2. Mark Tracking vs Digital Image Correlation

The Mark Tracking and the Digital Image Correlation techniques are suitable for measurements in the walls and in the pilot steel ladle. The mark tracking presents some advantages: *i)* lack of sensitivity to luminosity variation; *ii)* easy to use; *iii)* less computational time. However, it is not able to deal with discontinuities in the sample. Digital Image Correlation is a full-field measurement technique, efficient and relatively cheap. Therefore, some accuracy tests are being made in order to determine which technique will be used.

3.4.3. Evaluation of accuracy

It is possible to determine the accuracy of the techniques numerically, however it is only through experimental results that reliable uncertainty and performances can be obtained. For this reason, a series of stability tests is being performed. First, these tests will be performed in reduced scale (ø10 cm), the accuracy and uncertainties will be determined in pixels. After, the results will be extrapolated to the industrial scale and confirmed experimentally.

3.4.4. Mark tracking at laboratory scale

3.4.4.1. Evaluation of displacement accuracy

A stability test was performed using the mark tracking technique in an aluminium disk with diameter of 100 mm and thickness of 5 mm. The test last 60 minutes and the acquisition of images was made every 30 seconds. No load (mechanical nor thermal) was applied and stereovision was used. The sample is presented in Figure 18.

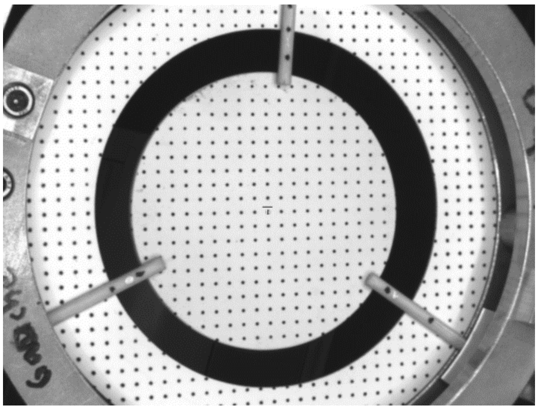

Figure 18: Aluminium disk - Stability Test.

The displacement of the central mark was evaluated using five methods available in *Deftac* software:

- *Suivi par Fenêtre*: Search for each spot in a rectangle. Fastest calculation but does not take into account the variation of brightness of the image or the fact that several spots can be found in the rectangle.
- *Suivi par Remplissage*: Search for each spot in a rectangle. Automatic modulation of the threshold intensity according to the brightness of the studied image and identification of the shape of each marker in order to avoid errors in the automatic choice of the marker.

- *Suivi par Fenêtre et modulation*: same as the first point, with an automatic modulation of the threshold intensity depending on the brightness of the image studied.
- *Suivi par Corrélation n/0*: Search for each task by correlation between state of charge and the initial state.
- *Suivi par Corrélation n/n-1*: Search for each task by correlation between state of charge and the previous state.

The displacements obtained for each technique are presented in Figure 19. The magnification factor is 13.29 for camera 1 and 13.32 for camera 2.

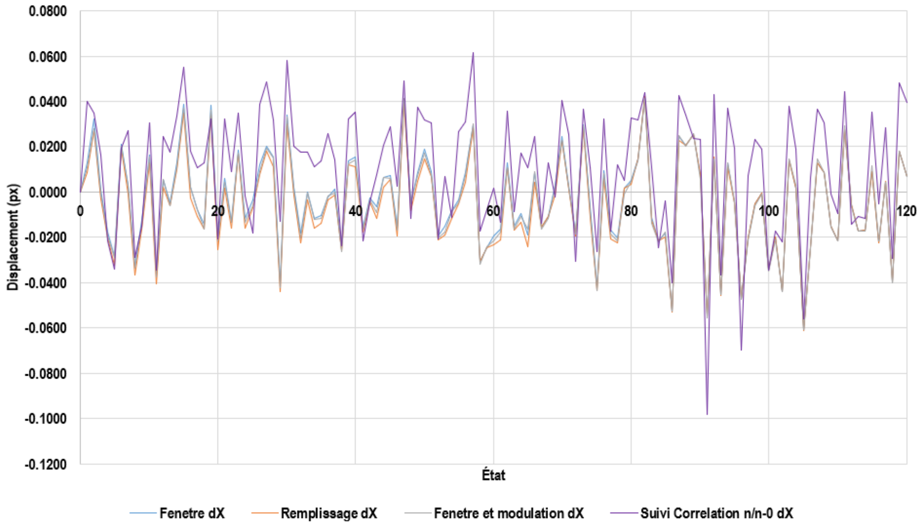

a)

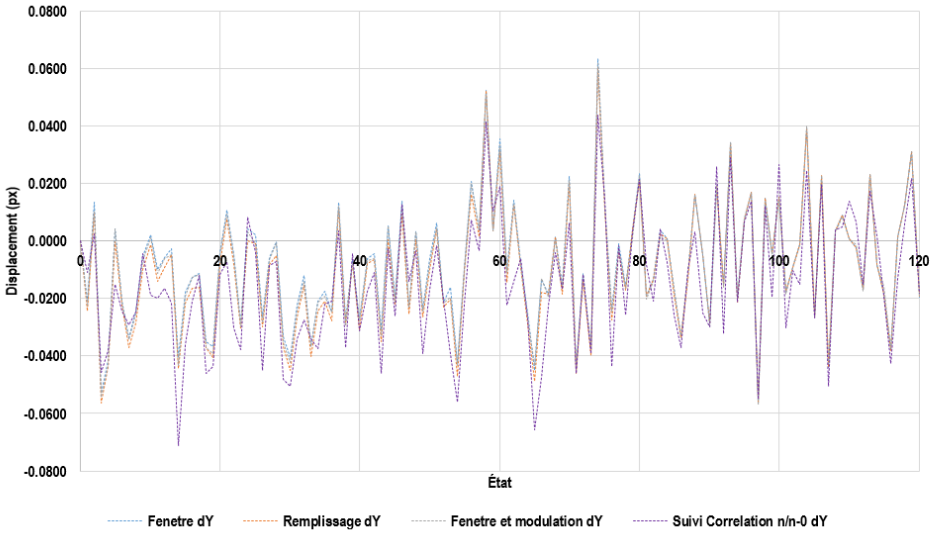

b)

Figure 19: Displacement of the central mark versus state: a) direction X; b) direction Y.

Based on these test results, it is possible to highlight the following points:

- As there was no luminosity variation, the results provided by the "*Suive par Fenêtre*", "*Suivi par Remplissage*" and "*Suivi par Fenêtre et Modulation*" are quite similar. For these techniques, the displacements at the central point varies from -0.06 to 0.06 px in direction X and from -0.057 to 0.063 px in direction Y along the test duration.
- The "*Suivi par Corrélation*" technique presented a bigger displacement at the central point. For the *n/0*, it was observed displacements from -0.098 to 0.061 px in direction X and from -0.071 to 0.044 px in direction Y. For the *n/n-1*, that was not presented in the graph, it was observed displacements -0.533 to 0.00 px in direction X and from 0 to 1.00 px in direction Y.

3.4.4.2. Evaluation of pitch size

To better understand the influence of the pitch (distance between markers) in the strains evaluation, a specific study was performed. As presented, the results provided by the "*Suivi par Fenêtre*", "*Suivi par Remplissage*" and "*Suivi par Fenêtre et Modulation*" are quite similar, therefore, the "*Suivi par Remplissage*" technique was used. The following distances were used (Figure 20):

- 5 mm;
- 10 mm;
- 15 mm.

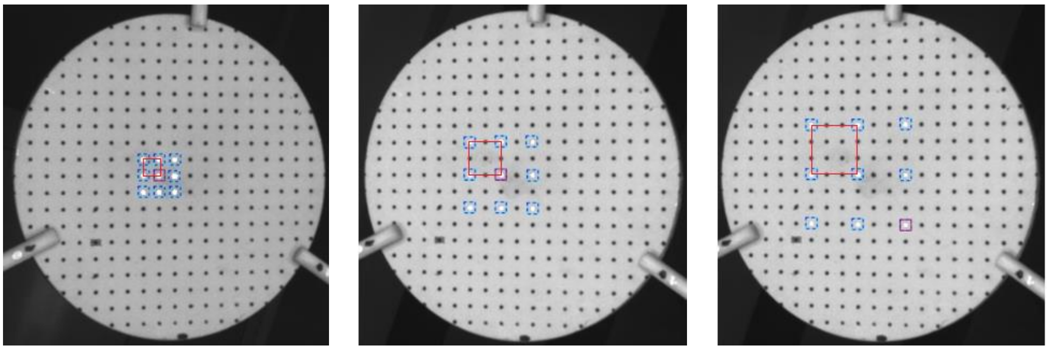

Figure 20: Makers position (a) 5 mm; (b) 10 mm; (c) 15 mm.

Figure 21 presents the strain at the centre of the sample. Based on the results, it is possible to conclude that:

- The noise in strains is bigger for the 5mm mesh, followed by the 10mm mesh. The 15mm mesh presented less noise than the others. So, as expected, increasing the distance between makers, decreases the noise.
- However, when dealing with the ATHORNA Device, where the strains are significantly higher at the centre of the specimen and decreases relatively fast, it is not possible to use a very large pitch, as it can jeopardize the measurment of strains.
- Thus, in order to reduce the noise without loss of accuracy the use of filters is necessary.

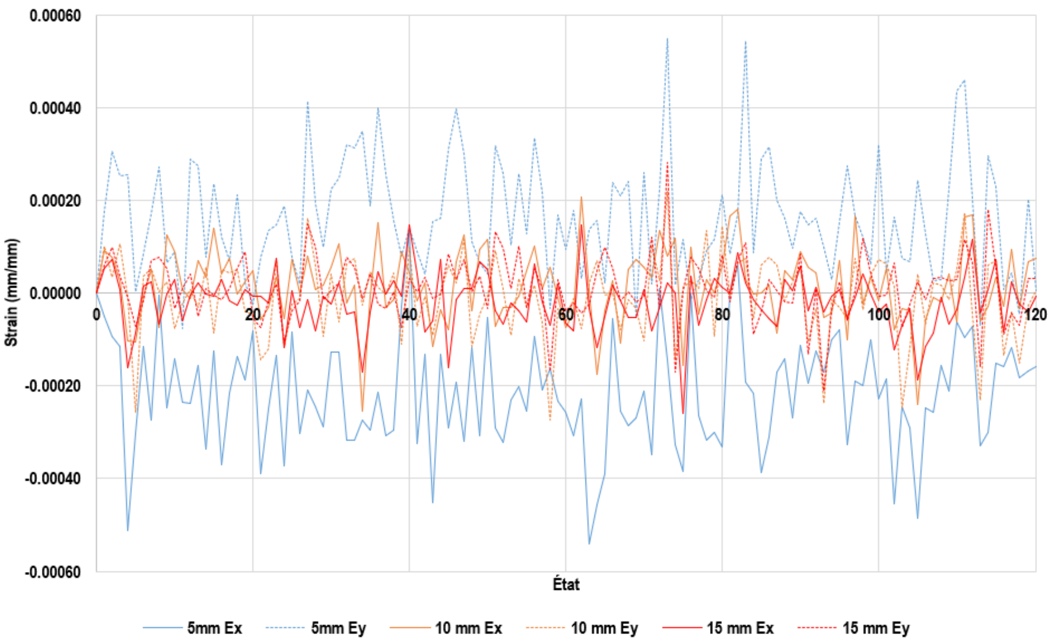

Figure 21: Strain in the centre of the specimen - Meshes #5mm, #10mm and #15mm.

3.4.4.3. Filtering results

The Savitzky-Golay filter is widely used to smooth experimental data, allowing an increase in accuracy without distorting the tendency of the data. A convolution process, successively fits sub-sets of adjacent data points, providing a *local average* in that subset, the result is an increase of the signal/noise ratio. Therefore, this filter provides a good reduction of noise, as presented in Figure 22. As can be seen in this figure:

- The filter provides a satisfactory smoothing of the data. The gross data presents a noise vary from -0.061 to 0.042 px. The 5-points smoothing vary from -0.040 to 0.030. The 7-points and 9-points smoothing vary from -0.0324 to 0.0281 px and -0.0247 to 0.0272 px, respectively.
- The Savitzky-Golay filter clearly increases the signal to noise ratio, improving the quality of the measurements.

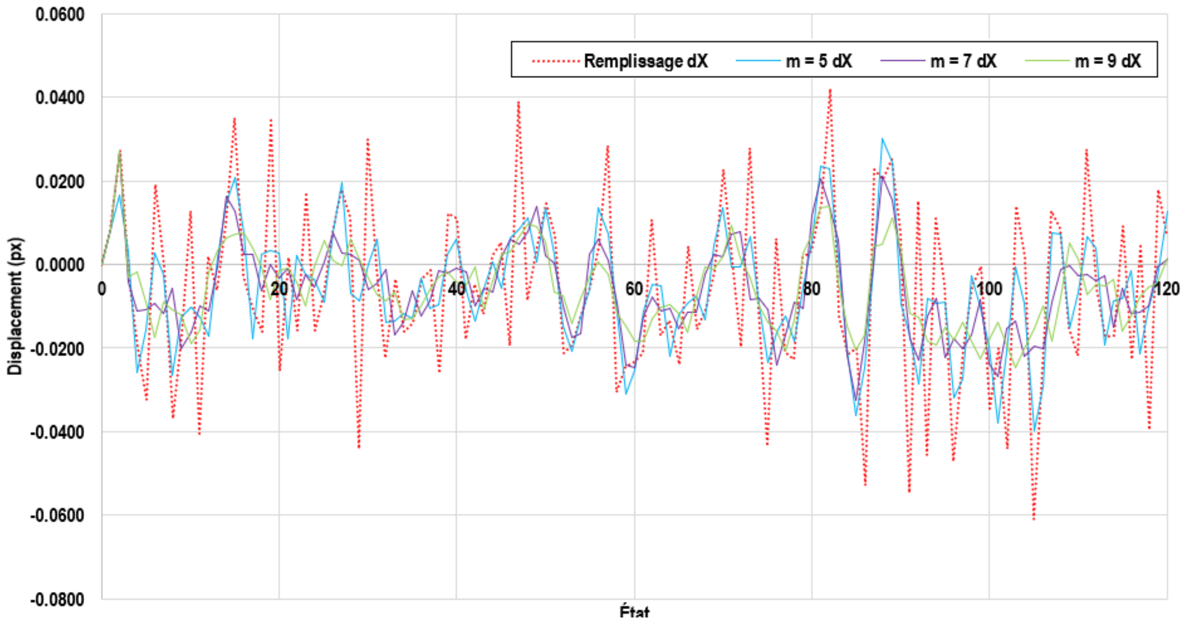

Figure 22: Data smoothing using Savitzky Golay filter - 5-points, 7-points and 9-points smoothing.

3.4.4.4. Digital Image Correlation at Laboratory Scale

The same stability test presented in 3.4.3.1 is being performed in an alumina spinel sample using Digital Image Correlation. The accuracy will be evaluated taking into account the size of the subsets, the use of digital filters and other parameters.

3.4.4.5. Full scale

Knowing the accuracy of the Mark tracking and DIC techniques for laboratory scale, it will be possible to extrapolate the uncertainties of the methods for the appropriated scale and evaluate which one will be most useful for the characterization of industrial vessels. These extrapolations will be confirmed by full scale stability and accuracy test in a plate with the dimensions of 1000x1000 mm.

3.4.5. Environmental conditions

Some environmental conditions may result in additional noise in the measurements:

- Temperature: temperature variations within the measurement environment during the test may leads to thermal expansion/contraction of camera supports, which can induce infinitesimal displacements between cameras. These in situ conditions may result in additional noise and loss of accuracy in the measurement system. Therefore, the cameras' supports shall be made in invar steel (FeNi36 or equivalent).
- Air convection: in order to avoid refractive index variation coming from irregular air convection adjacent to measured faces, the acquisition time shall be increased and some fans may be used between the cameras and the sample.
- Luminosity changes: an external source of light (such as LED lights) shall be used, aiming to avoid luminosity variations.
- Vibrations: the vibration levels shall be reduced to a minimum.

3.5. Thermal measurements

Temperature is a fundamental parameter in high temperature processes, and it must be controlled carefully. Each lining is composed of different materials with specific properties, which are temperature dependant. This means that the properties measured on a brick at room temperature are not the same as on a brick in service conditions. The acquisition of the temperature field is therefore of paramount importance. Thermal measurements in industrial conditions will be carried out with the help of thermocouples and an infrared camera.

The use of this equipment is crucial for two reasons:

- Monitoring and optimization of steel production;
- Improving workplace security.

In service condition, ladles present two types of temperature gradients (Figure 23):

- Across the lining (horizontally, from the contact layer out to the steel shell) due to the presence of the hot liquid steel;
- Along the lining (vertically, from top to bottom) which is also influenced from the contact with different liquids (slag or steel).

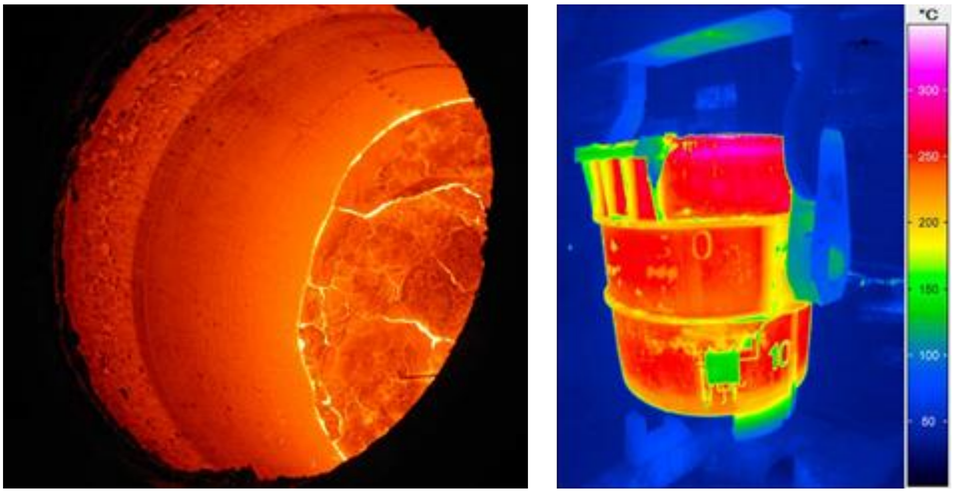

a) b)

Figure 23: Temperatures levels within a steel ladle: a) refractory internal surface of the ladle; b) temperature of the steel shell outside surface measured by an infrared camera.

Thermocouples will help monitoring the evolution of these gradients. K type will be used: Nickel-Chromium / Nickel-Alumel (nickel + aluminium + silicon alloy), being the most common and widely used. This is due to the fact they are inexpensive, accurate, reliable, and have a wide temperature range. The maximum temperature is around 1260°C with an accuracy of +/- 2.2°C.

They will be inserted in all the linings (working, safety and insulation) in different locations (Figure 24). To insert the thermocouples, holes will be drilled into the refractories. Marker pens and duct tape will assist in keeping thermocouples in place and can be used to plot where sub level thermocouples have previously been installed. Careful attention will be paid during the installation in order to ensure no overlapping of thermocouples as this could cause crushing of the equipment and change location of recording. At the same time, a “working document” will be filled in with the information of which number thermocouple is in which position in order to clarify results interpretation.

Furthermore, to increase the lifetime of refractory linings and operating safety, a laser scanner will be used. The LaCam profile measuring system has been developed for non-contact measurements of hot refractory linings in metallurgical reactors and transport vessels [4]. This kind of equipment allows controlling the variation of thickness of the bricks in hot conditions. The system consists of a 3D laser profile measurement head mounted on top of a cooled movable boom, a cooling system, an automated mechanical manipulator and an industrial PC station. Infrared laser pulses are sent to the wall and the bottom of the ladle. The accuracy of the measurement is impacted by the spot size of the laser beam, which depends on the laser beam´s angle of incidence. In addition to distance measurements, a dedicated channel is also able to measure the local temperature of each point leading to a global temperature map of the entire internal surface of the ladle. An issue can be the shadowed area below the ladle mouth, which is not accessible for the laser beam when measurements are managed from the outside. This disadvantage has an impact on measurability of the slag zone, a very important area in ladle lining relating to the risk of a breakthrough. To overcome the above problem, laser head system has been developed. The special cooling system and application of specialized heat protection materials, the easy yet sturdy construction, and the fast measurement time enable the laser head to be immersed into the hot ladle with ambient temperatures of more than 1,000°C without being damaged (*Figure 25*). The whole measurement sequence runs automatically and takes less than three minutes.

a) b)

Figure 24: Installation of thermocouples on steel ladle lining: a) front view; b) top view.

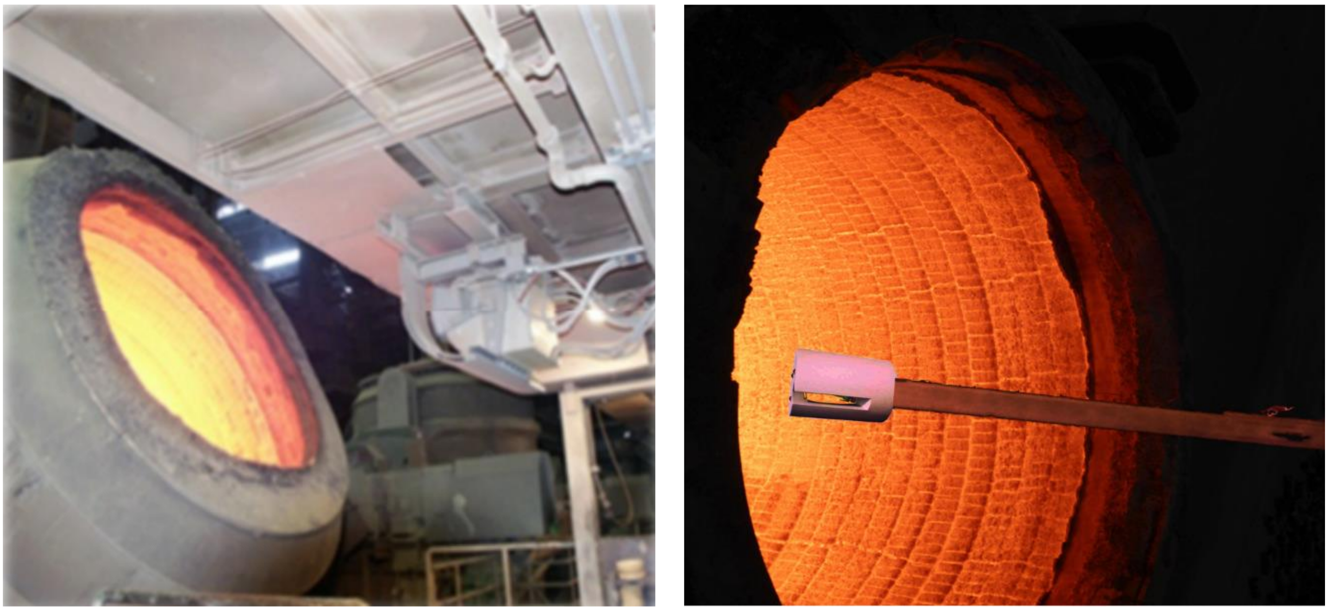

a) b)

Figure 25: Laser scanner measures on the internal surface of the ladle:
a) from the outside the steel ladle; b) laserhead being into the ladle [15].

4. Conclusions and final considerations

This document summarizes the tests to be performed for the thermomechanical characterization and monitoring of the refractory masonry subsystems, including the suitable acquisition equipment and techniques. This deliverable is the output of the “Task 1.5 - Devices for validation on masonry vessels” as a task of “WP1 - Improvements of measurements tools”.

Section 2 describes the different experimental campaigns defined to properly characterize the thermomechanical behaviour of refractory masonry under different boundary conditions. This includes tests on: a) compressive behaviour of bricks (at both ambient and elevated temperatures); b) characterization of the joints; c) uniaxial compression behaviour of masonry walls (at elevated temperatures) and d) bi-axial behaviour of masonry walls (at elevated temperatures). Section 3 described the development of the 3D pilot scale steel ladle and the different alternative techniques that can be used to measure its behaviour during the different laboratory tests.

As presented in this document, there are many techniques available for the evaluation of temperatures, displacements and strains. However, when dealing with the service temperatures of refractories, these techniques may not be completely suitable and some improvements will certainly be necessary. Due to the scale of the masonry vessels, some additional evaluation of the methods will also be necessary.

In conclusion, the improvements of measurements tools performed within WP1, including the “Tasks 1.1 - Thermal instrumentation”, “Task 1.2 - Strain Instrumentation” and “Task 1.4 - Devices for thermomechanical characterization” are increasing the current knowledge and allowing the development and validation of innovative techniques presented in this report.

5. References

[1] Lopes FR, Pereira JM, Rodrigues JP, Lourenço PB, Análise experimental de uma parede de alvenaria estrutural de blocos de concreto de três células em situação de incêndio. Concreto & Construções. 89, 2018, pp. 22-30.

[2] Prietl T, Ermittlung materialspezifischer Kennwerte von feuerfesten Werkstoffen und Zustellungen unter uni- und biaxialen Lastbedingungen für die Nichteisenmetallindustrie. PhD thesis at the University of Leoben, Leoben, 2006.

[3] Triessnig A, Studnicka H, Prietl T, Determination of Thermo-Mechanical Properties at the RHI Refractories Technology Center Leoben. RHI Bulletin 1, 2006.

[4] Rolf Lamm, Laser Measurement System for the Refractory Lining of Hot Torpedo Ladles. A Publication of the Association for Iron & Steel Technology. AISTech, 2013.

[5] N. Bretagne, V. Valle, J.C. Dupre. Development of the marks tracking technique for strain field and volume variation measurements. NDT&E International 1-9, 2004.

[6] Besnard, G., Hild, F. & Roux, S. Finite-Element Displacement Fields Analysis from Digital Images: Application to Portevin-Le Châtelier Bands. Exp. Mech. 46, 2006, 789-803.

[7] Mandelli A, Fassi F, Perfetti L, Polari C. Testing different survey techniques to model architectonic narrow spaces. Int Arch Photogrammetry Remote Sens Spatial Inf Sci - ISPRS Arch 2017; 42(2W5), 2017, 505–11.

[8] Napolitan, R., Glisic, B. Methodology for diagnosing crack patterns in masonry structures using photogrammetry and distinct element modeling. Engineering Structures, Volume 181, 2019, 519-528,

[9] Wang C-H, Mills JP, Miller PE. Automated low-cost photogrammetry for flexible structure monitoring. Int Arch Photogrammetry Remote Sens Spatial Inf Sci, 39, 2012, 393-398.

[10] Sapirstein P. Photogrammetry as a tool for architectural analysis: the digital architecture project at olympia. In: Archaeological research in the digital age. vol. 1, 2014, 129-139.

[11] Patias P, Santana Quintero M. Introduction to heritage documentation. ISPRS Int Arch Photogrammetry Remote Sens Spatial Inf Sci;XXXVIII, 1, 2009, 9-13.

[12] Percy K, Ward S, Santana Quintero M, Morrison T. Integrated digital technologies for the architectural rehabilitation & conservation of beinn bhreagh hall & surrounding site, Nova Scotia, Canada. ISPRS Ann Photogrammetry Remote Sens Spatial Inf Sci 2015;II-5/W3 (September), 2015, 235-241.

[13] Shrestha S, Reina Ortiz M, Gutland M, Napolitano R, Morris IM, Santana Quintero M, et al. Digital recording and non-destructive techniques for the understanding of structural performance for rehabilitating historic structures at the Kathmandu valley after gorkha earthquake 2015. ISPRS Ann Photogrammetry Remote Sens Spatial Inf Sci, 4, 2017; 243-250.

[14] Troisi, S., Baiocchi, V., Del Pizzo, S., Giannone, F., A prompt methodology to georeference complex hypogea environments. In: Int. Arch. Photogramm. Remote Sens. Spatial Inf. Sci., Nafplio, Greece, Vol. XLII-2/W3, 2017, 639-644.

[15] Rolf Lamm, Stefan Kirchhoff, Optimization of ladle refractory lining, gap and crack detection, lining surface temperature and sand-filling of the ladle-taphole by means of a 3D-laserprofile-measurement system that is immersed into a hot ladle to evaluate the entire condition. Minteq International GmbH - Ferrotron Division.